Published in final edited form as:
Curr Biol. 2008 September 9; 18(17): 1295–1299. doi:10.1016/j.cub.2008.07.090.

Extracellular matrix rigidity promotes invadopodia activity

Nelson R. Alexander[1,§], **Kevin M. Branch**[1], **Aron Parekh**[1], **Emily S. Clark**[1], **Izuchukwu C. Iwueke**[1], **Scott A. Guelcher**[2], and **Alissa M. Weaver**[1,3]

1*Department of Cancer Biology, Vanderbilt University, Nashville, TN 37232, USA*

2*Department of Chemical Engineering, Vanderbilt University, Nashville, TN 37232, USA*

3*Department of Pathology, Vanderbilt University, Nashville, TN 37232, USA*

Summary

Invadopodia are actin-rich subcellular protrusions with associated proteases used by cancer cells to degrade extracellular matrix (ECM) [1]. Molecular components of invadopodia include branched actin assembly proteins, membrane trafficking proteins, signaling proteins and transmembrane proteinases[1]. Similar structures exist in nontransformed cells, such as osteoclasts and dendritic cells, but are generally called podosomes and are thought to be more involved in cell-matrix adhesion than invadopodia [2–4]. Despite intimate contact with their ECM substrates, it is unknown whether physical or chemical ECM signals regulate invadopodia function. Here, we report that ECM rigidity directly increases both the number and activity of invadopodia. Transduction of ECM rigidity signals depends on the cellular contractile apparatus [5–7], as inhibition of nonmuscle myosin II, myosin light chain kinase, and Rho kinase all abrogate invadopodia-associated ECM degradation. Whereas myosin IIA, IIB, and phosphorylated myosin light chain do not localize to invadopodia puncta, active phosphorylated forms of the mechanosensing proteins p130Cas (Cas) and focal adhesion kinase (FAK) are present in actively degrading invadopodia and the levels of phospho-Cas and phospho-FAK in invadopodia are sensitive to myosin inhibitors. Overexpression of Cas or FAK further enhances invadopodia activity in cells plated on rigid polyacrylamide substrates. Thus, in invasive cells, ECM rigidity signals lead to increased matrix-degrading activity at invadopodia, via a myosin II-FAK/Cas pathway. These data suggest a potential mechanism, via invadopodia, for the reported correlation of tissue density with cancer aggressiveness.

Keywords

Invadopodia; Extracellular matrix; rigidity; mechanotransduction; cell contractility; tumor invasion

Results and Discussion

ECM serves both a signaling and structural role in tissues. In most cases, ECM is considered to function as a barrier to cell movements and in fact degradation by invadopodia constitutes an important mechanism to cross those barriers. However, when we tested the role of ECM density on invadopodia function, we unexpectedly found that denser gelatin substrates led to

Correspondence to: Alissa M. Weaver.

§Current address: Ventana Medical Systems, Inc, Tucson, AZ 85755, USA

an increase in both the number and ECM-degrading capacity of invadopodia (Fig 1). For these studies, CA1d breast carcinoma cells were cultured overnight on ECM substrates of 0.5%–5% gelatin, overlaid with FITC-labeled fibronectin (FN), followed by fixation and staining with rhodamine-labeled phalloidin to identify actin-rich invadopodia puncta. As shown in Fig 1, cells cultured on ECM substrates with a low percentage of gelatin (0.5%) produced fewer invadopodia and degraded less FN than cells grown on ECMs with higher percentages of gelatin. The largest increase in invadopodia number and FN degradation is evident when the percentage of gelatin is increased from 2.5% to 5% (Fig 1B). Similar results were seen using FITC-gelatin instead of FITC-FN/unlabeled gelatin (data not shown).

Increasing the density of the ECM is likely to increase substrate rigidity, which has been shown to affect a variety of cell functions including migration and cell lineage specification [5–8]. To test whether ECM substrates made with increased gelatin concentrations were more rigid, we measured viscoelastic properties of gelatin gels on a TA Instruments AR-G2 rheometer at 37° C (Fig 1C). Gels were compressed between a heated Peltier plate and a 25-mm upper plate and subjected to an oscillating shear strain. The storage and loss moduli were measured as a function of frequency, which was varied from 0.1 – 10 Hz. The storage modulus is related to the energy that is stored elastically when the gel is subjected to a small oscillatory shear deformation. As expected, increasing the gelatin concentration increases the storage modulus, most dramatically when the percentage of gelatin is increased from 2.5% to 5% (Fig 1C). These data suggest that rigidity may play a causative role in promoting invadopodia activity.

In addition to altering ECM rigidity, increasing the gelatin concentration in invadopodia substrates could increase the number of integrin ligands. Thus, increased ECM-integrin signaling might promote invadopodia formation and function through a mechanism that is unrelated to ECM rigidity but rather due to increased integrin ligand availability or proximity [9]. To remove this confounding factor, we cultured cells using the same conditions as the previous experiment, except for plating on hard (3300 Pascals) or soft (360 Pascals) polyacrylamide (PA) gels that were coated with identical concentrations of gelatin (1%), followed by FITC-Fn. Interestingly, cells cultured on hard PA gels produce more invadopodia and degrade more ECM than cells cultured on soft PA gels (Fig 2). Similar results were seen with FITC-gelatin coating (data not shown), and coating with gelatin or fibronectin/gelatin has little effect on the storage modulus of PA gels in rheology experiments (Supp Fig 1). These data provide strong evidence that ECM rigidity promotes invadopodia formation and function.

Cells are thought to sense ECM rigidity through integrin-actomyosin interactions, leading to generation of intracellular tensile forces through contraction of non-muscle myosin II (nm-myosin II) [5,6]. To test the role of myosin II in invadopodia function, chemical inhibitors of either myosin II (blebbistatin) or its upstream activator myosin light chain kinase (ML-7) were added to cells two hours after plating. In either case, inhibition of myosin II activity results in a dose dependent decrease in ECM degradation (Fig 3A,B). Inhibition of Rho kinase, another molecule that promotes cellular contractility through effects on myosin light chain phosphorylation, also prevents invadopodia-mediated ECM degradation (Supp Fig 2). Interestingly, numerous small puncta that label with the invadopodia markers actin and cortactin are still present at the ventral surface of inhibitor-treated cells and weakly protrude into the layer of labeled FN; however they are smaller and not associated with ECM degradation (Fig 3A,E). Although the number of total invadopodia (cortactin-, actin-positive puncta) is variable with inhibitor treatment (red bars, Fig 3C), the number of functional, ECM-degrading invadopodia (cortactin-, actin-positive puncta with associated ECM degradation) is consistently decreased with drug treatment (blue bars, Fig 3C). These data suggest that myosin-based transmission of rigidity signals may promote maturation rather than formation of invadopodia. We also noticed changes in mean cell area with blebbistatin and ML-7 treatment; however the changes were in opposite directions and unlike in 2-dimensional systems [9] mean

cell area did not change significantly in the invadopodia system with changes in matrix rigidity (Supp Fig 3).

Despite the observed defect in invadopodia maturation and ECM degradation with inhibitors of myosin II or its upstream activators, neither myosin IIA, IIB, nor phosphor-myosin light chain (pMLC) localized to invadopodia (Supp Fig 4). In fact, there was a notable absence of myosin staining within the puncta. Interestingly, however, in 39.6% of cells myosin IIA localized in a ring-like structure around invadopodia (Supp Fig 4A, yellow arrow, see zoom). This localization is reminiscent of the rings of adhesion proteins found around actin cores in podosomes [2, 3]. By contrast, there is either weak or no apparent localization of myosin IIB or pMLC around invadopodia (Supp Fig 4, red arrows). These data indicate that myosin contraction is likely to occur outside of the invadopodia puncta structure, leading however to increased invadopodia function.

One mechanism that has been identified for transduction of mechanical/contractile forces into signals is mechanosensitive alterations in the structure of proteins such as p130Cas [10], and potentially focal adhesion kinase (FAK) [11], in response to myosin II pulling of actin-attached adhesion complexes [12]. Mechanical stretching of p130Cas has been shown to extend the substrate domain, allowing phosphorylation at multiple sites that are key for integrin signaling pathways [10,13]. Immunostaining with a phosphospecific antibody that recognizes a site in the Cas substrate domain, pY165, reveals that it is concentrated at invadopodia, and colocalizes with areas of ECM degradation (Fig 4A). Z-section reconstructions indicate that pY165-Cas is present throughout invadopodial protrusions. Thus far, a direct effect of mechanical stretching on the molecular conformation of FAK has only been theoretically predicted from molecular dynamics simulations [11]. However, tyrosine phosphorylation of focal adhesion kinase (FAK) increases in cells subjected to mechanical strain [14–16] and a blocking antibody that targets the autophosphorylation site tyrosine 397 inhibits flow-induced dilatation of coronary arterioles [17]. Confocal imaging of cells stained with a phosphospecific antibody against pY397-FAK also reveals staining throughout invadopodial protrusions (Fig 4B, Z-analysis). Between FAK and Cas, there was a greater tendency to find strong staining of p130Cas at invadopodia and strong staining of FAK at focal adhesions (where they occurred), but both molecules were found in both structures. Immunostaining for total FAK and Cas also demonstrated localization to invadopodia, albeit weaker than that of phosphorylated FAK and Cas (data not shown).

To test whether the phosphorylation of invadopodia-localized FAK and Cas can be altered by contractility, cells were treated with myosin inhibitors and fixed and stained for actin filaments and antibodies specific for either pY397-FAK or pY165-Cas. The intensity of phosphorylated FAK or Cas was quantitated using a predefined 4×4 pixel wide box in the center of actively degrading invadopodia. Consistent with a role in mechanosensing, treatment of cells with blebbistatin or ML-7 led to a significant decrease in the intensity of phosphorylated FAK and Cas in the few actively degrading invadopodia that were present (Fig 4C). By contrast, in non-degrading actin puncta from the same images there was no effect of blebbistatin or ML-7 on phosphoFAK or phosphoCas intensity compared with DMSO-treated controls (Fig 4C). We also expressed exogenous FAK and p130Cas in CA1d cells at 3–4-fold endogenous levels (Fig 4D), which had no obvious effect on the expression of other cell proteins, with the possible exception of a ~60 kDa band in the FAK-OE cells (Supp Fig 5). Interestingly, expression of either FAK or Cas increases invadopodia-associated degradation, compared with controls, particularly on rigid substrates (Fig 4D). Cas is consistently more robust than FAK in promoting invasiveness, although this may be due to slightly higher expression levels (Fig 4D). These data are consistent with a role for FAK and Cas in rigidity-promoted invadopodia activity; future studies are required to determine the mechanism as well as the role of FAK and Cas phosphorylation in this process.

Our results indicate that the cellular processes regulating ECM degradation are instructed by the physics of the surrounding microenvironment. Because nm-myosin II is noticeably absent from invadopodial protrusions, contraction does not appear to occur within these structures. Based on the presence of phosphorylated forms of the mechanosensing proteins FAK and p130Cas in invadopodia and the responsiveness to myosin inhibitors, we speculate that contractile forces may be transmitted through cellular actin fibers to invadopodia to activate these and other mechanosensing proteins. Such long-range activation of mechanosensing proteins is consistent with a study in which long-range and directional activation of a src kinase-based FRET reporter occurred in response to laser tweezer-applied forces on fibronectin-coated beads [18]. Alternatively, activation of proteins such as FAK and Cas could occur outside of invadopodia, with subsequent transport to invadopodia. In addition, we cannot rule out the possibility of external enhancement of cellular processes such as signaling or membrane trafficking that promote invadopodia activity. Interestingly, myosin IIA sometimes localizes in a ring around invadopodia, similar to the ring of adhesion proteins seen around the actin core in podosomes [3]. The ring or whole cell population of myosin IIA could provide the force to transmit rigidity signals from the matrix.

In noninvasive cells, focal adhesions are the primary centers of mechanotransduction as the point where contractile actin stress fibres connect with integrins and integrin-associated signaling proteins such as src kinase, FAK and p130Cas [14]. In normal cells that need to remodel ECM or cross tissue barriers, podosomes are the primary adhesive structures and contain both focal adhesion and branched actin assembly proteins [2,3]. Invadopodia and podosomes share many common molecular components; however, the link to adhesion molecules is much less well established for invadopodia than for podosomes [1–3,19]. Interestingly, expression of p130Cas in src-transformed fibroblasts was previously shown to promote the formation of large ring-like podosome structures, activation of matrix metalloproteinase 2, invasion through Matrigel-coated transwell chambers and experimental metastasis; however other noninvasive src-dependent phenotypes, such as anchorage-independent growth were unaffected [20,21]. These Cas-dependent phenotypes required intact tyrosine residues in the mechanosensitive substrate domain [10,21]. FAK may promote invadopodia formation [22] and has been tied in separate studies to mechanosensing [12,14–17]. In light of our results that ECM rigidity promotes invadopodia activity, that contractility affects the phosphorylation of FAK and Cas in invadopodia and that expression of p130Cas and FAK increases invadopodia activity on rigid substrates, we speculate that in invasive cancer cells ECM rigidity may be one important input to p130Cas and FAK to promote cellular invasion. It is also likely that other molecules not tested in this study are involved in the invasive response to ECM rigidity.

In cancer, tumor cells experience increasing tissue rigidity during tumor development and progression [23–25]. Our data suggest that one response to rigid tissue environments is upregulation of the production and function of invadopodia. Indeed, increased breast density on mammograms is correlated with increased risk for invasive behavior of breast cancers, such that breast density measurements improve the predictiveness of other clinical staging/prognostic parameters [26,27]. Our data complement recent reports demonstrating altered morphologies and signaling through Rho and Rho kinase of breast epithelial cells in rigid 3D cultures [24,28], and provide a novel mechanism of increased invasiveness as well as indicating potential mechanotransduction targets for anti-invasive therapies.

Supplementary Material

Refer to Web version on PubMed Central for supplementary material.

Acknowledgements

We thank Drs. Donna Webb and Vito Quaranta for critical reading of the manuscript and Dr. Steve Hanks for provision of the LZRS-MS-GFP, LZRS-MS-CAS and LZRS-MS-FAK vectors. Funding was provided by NIH K22CA109590 and R01GM075126 to AMW and by NCI U54CA113007 to the Vanderbilt Integrative Cancer Biology Center, and by the Vanderbilt University School of Engineering to SAG. NRA was funded by NCI training grant T32CA09592. Rheology experiments were performed at the Center for Nanophase Materials Science at Oak Ridge National Laboratory under User Proposal CNMS2006-069.

References

1. Weaver AM. Invadopodia: specialized cell structures for cancer invasion. Clin Exp Metastasis 2006;23:97–105. [PubMed: 16830222]
2. Linder S. The matrix corroded: podosomes and invadopodia in extracellular matrix degradation. Trends Cell Biol 2007;17:107–117. [PubMed: 17275303]
3. Linder S, Aepfelbacher M. Podosomes: adhesion hot-spots of invasive cells. Trends Cell Biol 2003;13:376–385. [PubMed: 12837608]
4. Burgstaller G, Gimona M. Actin cytoskeleton remodelling via local inhibition of contractility at discrete microdomains. J Cell Sci 2004;117:223–231. [PubMed: 14676275]
5. Clark K, Langeslag M, Figdor CG, van Leeuwen FN. Myosin II and mechanotransduction: a balancing act. Trends Cell Biol 2007;17:178–186. [PubMed: 17320396]
6. Giannone G, Sheetz MP. Substrate rigidity and force define form through tyrosine phosphatase and kinase pathways. Trends Cell Biol 2006;16:213–223. [PubMed: 16529933]
7. Pelham RJ Jr, Wang Y. Cell locomotion and focal adhesions are regulated by substrate flexibility. Proc Natl Acad Sci U S A 1997;94:13661–13665. [PubMed: 9391082]
8. Guo WH, Frey MT, Burnham NA, Wang YL. Substrate rigidity regulates the formation and maintenance of tissues. Biophys J 2006;90:2213–2220. [PubMed: 16387786]
9. Engler A, Bacakova L, Newman C, Hategan A, Griffin M, Discher D. Substrate compliance versus ligand density in cell on gel responses. Biophys J 2004;86:617–628. [PubMed: 14695306]
10. Sawada Y, Tamada M, Dubin-Thaler BJ, Cherniavskaya O, Sakai R, Tanaka S, Sheetz MP. Force sensing by mechanical extension of the Src family kinase substrate p130Cas. Cell 2006;127:1015–1026. [PubMed: 17129785]
11. Mofrad MR, Golji J, Abdul Rahim NA, Kamm RD. Force-induced unfolding of the focal adhesion targeting domain and the influence of paxillin binding. Mech Chem Biosyst 2004;1:253–265. [PubMed: 16783922]
12. Frey MT, Tsai IY, Russell TP, Hanks SK, Wang YL. Cellular responses to substrate topography: role of myosin II and focal adhesion kinase. Biophys J 2006;90:3774–3782. [PubMed: 16500965]
13. Fonseca PM, Shin NY, Brabek J, Ryzhova L, Wu J, Hanks SK. Regulation and localization of CAS substrate domain tyrosine phosphorylation. Cell Signal 2004;16:621–629. [PubMed: 14751547]
14. Katsumi A, Orr AW, Tzima E, Schwartz MA. Integrins in mechanotransduction. J Biol Chem 2004;279:12001–12004. [PubMed: 14960578]
15. Wozniak MA, Modzelewska K, Kwong L, Keely PJ. Focal adhesion regulation of cell behavior. Biochim Biophys Acta 2004;1692:103–119. [PubMed: 15246682]
16. Yano Y, Geibel J, Sumpio BE. Tyrosine phosphorylation of pp125FAK and paxillin in aortic endothelial cells induced by mechanical strain. Am J Physiol 1996;271:C635–C649. [PubMed: 8770005]
17. Koshida R, Rocic P, Saito S, Kiyooka T, Zhang C, Chilian WM. Role of focal adhesion kinase in flow-induced dilation of coronary arterioles. Arterioscler Thromb Vasc Biol 2005;25:2548–2553. [PubMed: 16195476]
18. Wang Y, Botvinick EL, Zhao Y, Berns MW, Usami S, Tsien RY, Chien S. Visualizing the mechanical activation of Src. Nature 2005;434:1040–1045. [PubMed: 15846350]
19. Weaver AM. Invadopodia. Curr Biol 2008;18:R362–R364. [PubMed: 18460310]
20. Brabek J, Constancio SS, Shin NY, Pozzi A, Weaver AM, Hanks SK. CAS promotes invasiveness of Src-transformed cells. Oncogene 2004;23:7406–7415. [PubMed: 15273716]

21. Brabek J, Constancio SS, Siesser PF, Shin NY, Pozzi A, Hanks SK. Crk-associated substrate tyrosine phosphorylation sites are critical for invasion and metastasis of SRC-transformed cells. Mol Cancer Res 2005;3:307–315. [PubMed: 15972849]

22. Hauck CR, Hsia DA, Ilic D, Schlaepfer DD. v-Src SH3-enhanced interaction with focal adhesion kinase at beta 1 integrin-containing invadopodia promotes cell invasion. J Biol Chem 2002;277:12487–12490. [PubMed: 11839732]

23. Krouskop TA, Wheeler TM, Kallel F, Garra BS, Hall T. Elastic moduli of breast and prostate tissues under compression. Ultrason Imaging 1998;20:260–274. [PubMed: 10197347]

24. Paszek MJ, Zahir N, Johnson KR, Lakins JN, Rozenberg GI, Gefen A, Reinhart-King CA, Margulies SS, Dembo M, Boettiger D, Hammer DA, Weaver VM. Tensional homeostasis and the malignant phenotype. Cancer Cell 2005;8:241–254. [PubMed: 16169468]

25. Plewes DB, Bishop J, Samani A, Sciarretta J. Visualization and quantification of breast cancer biomechanical properties with magnetic resonance elastography. Phys Med Biol 2000;45:1591–1610. [PubMed: 10870713]

26. Barlow WE, White E, Ballard-Barbash R, Vacek PM, Titus-Ernstoff L, Carney PA, Tice JA, Buist DS, Geller BM, Rosenberg R, Yankaskas BC, Kerlikowske K. Prospective breast cancer risk prediction model for women undergoing screening mammography. J Natl Cancer Inst 2006;98:1204–1214. [PubMed: 16954473]

27. Chen J, Pee D, Ayyagari R, Graubard B, Schairer C, Byrne C, Benichou J, Gail MH. Projecting absolute invasive breast cancer risk in white women with a model that includes mammographic density. J Natl Cancer Inst 2006;98:1215–1226. [PubMed: 16954474]

28. Wozniak MA, Desai R, Solski PA, Der CJ, Keely PJ. ROCK-generated contractility regulates breast epithelial cell differentiation in response to the physical properties of a three-dimensional collagen matrix. J Cell Biol 2003;163:583–595. [PubMed: 14610060]

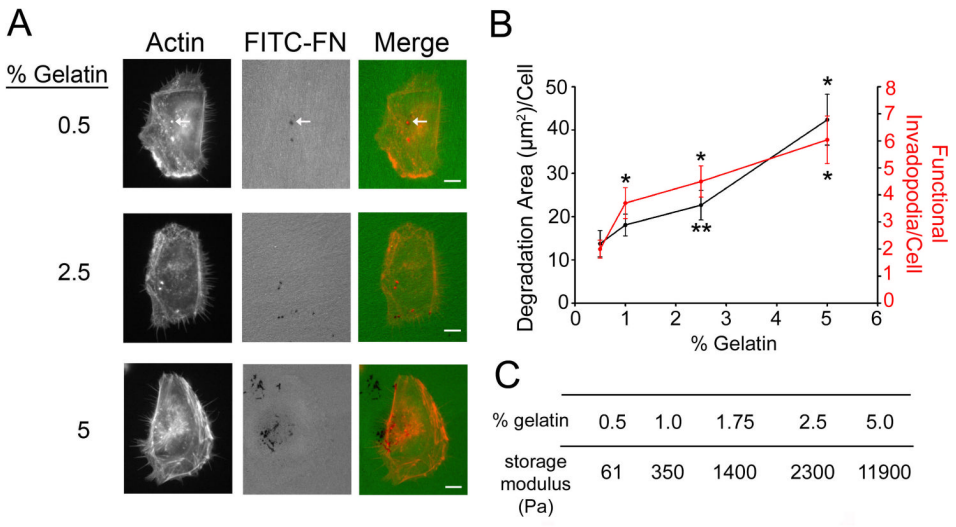

Figure 1. Increased density of gelatin cushions regulates invadopodia functions

A. Wide field fluorescence images of invadopodia in CA1D cells cultured on FITC-FN/gelatin cushions with increasing gelatin percentage. Scale bars = 10 μm. **B**. Quantification of ECM degradation area/cell and number of functional invadopodia/cell (actin puncta associated with degradation sites). Data are represented as mean+/−standard error (SE) * indicates p value < 0.05, ** indicates p<0.06, compared with 0.5% gelatin. n=3 **C**. The storage moduli of gelatin cushions were measured by rheology, using a TA Instruments AR-G2 rheometer at 37°C using a 25 mm circular head. The mean values are reported from 2 independent experiments performed in triplicate.

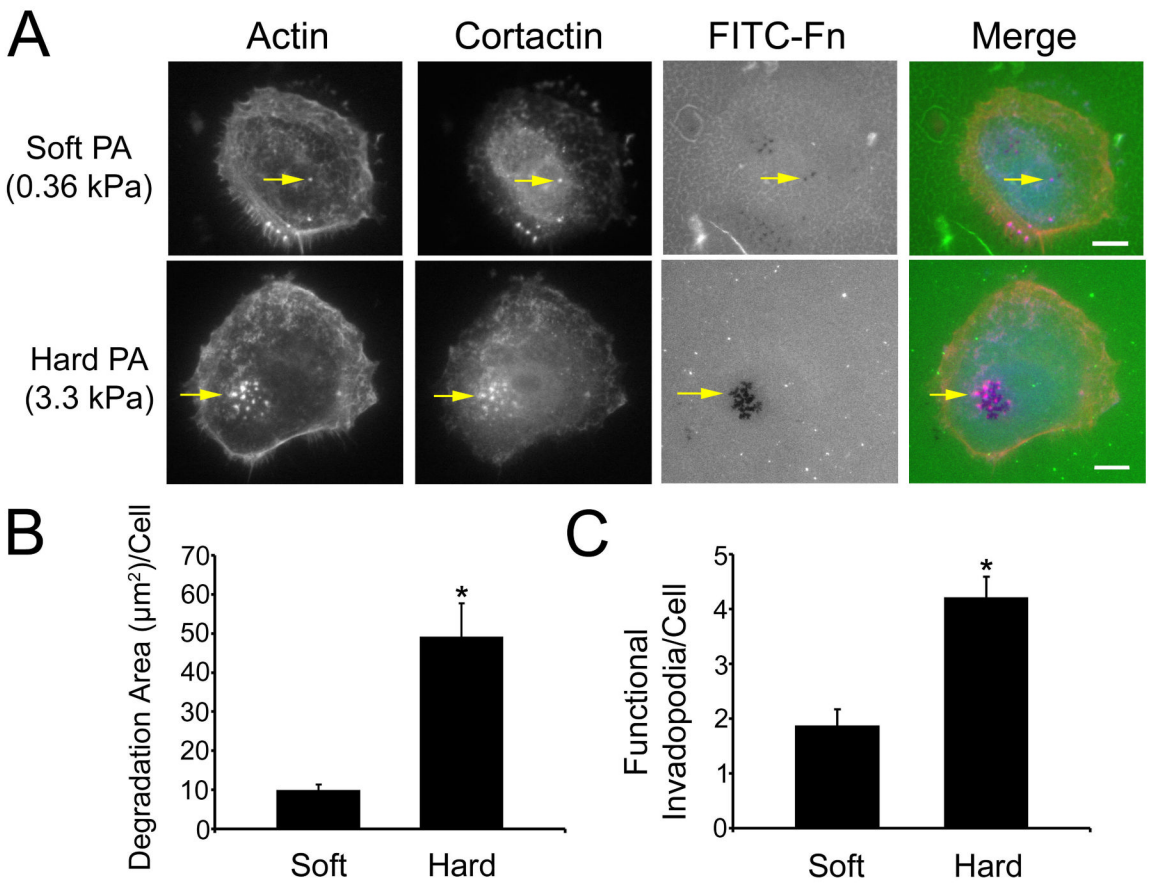

Figure 2. ECM rigidity promotes invadopodia formation and function

A. Images of cells cultured on FITC-Fn/1% gelatin-coated polyacrylamide (PA) gels with different rigidities ("Soft" or "Hard"). Rigidity numbers reported for PA gels are in kiloPascals (kPa) and are storage moduli, empirically determined. Arrows point to example invadopodia. **B**. Quantification of invadopodia degradation area/cell. **C**. Number of F-actin/cortactin dual staining invadopodia associated with ECM degradation ("Functional Invadopodia") per cell. Data are represented as mean+/−SE. * indicates p value < 0.05 Scale bars = 10 μm.

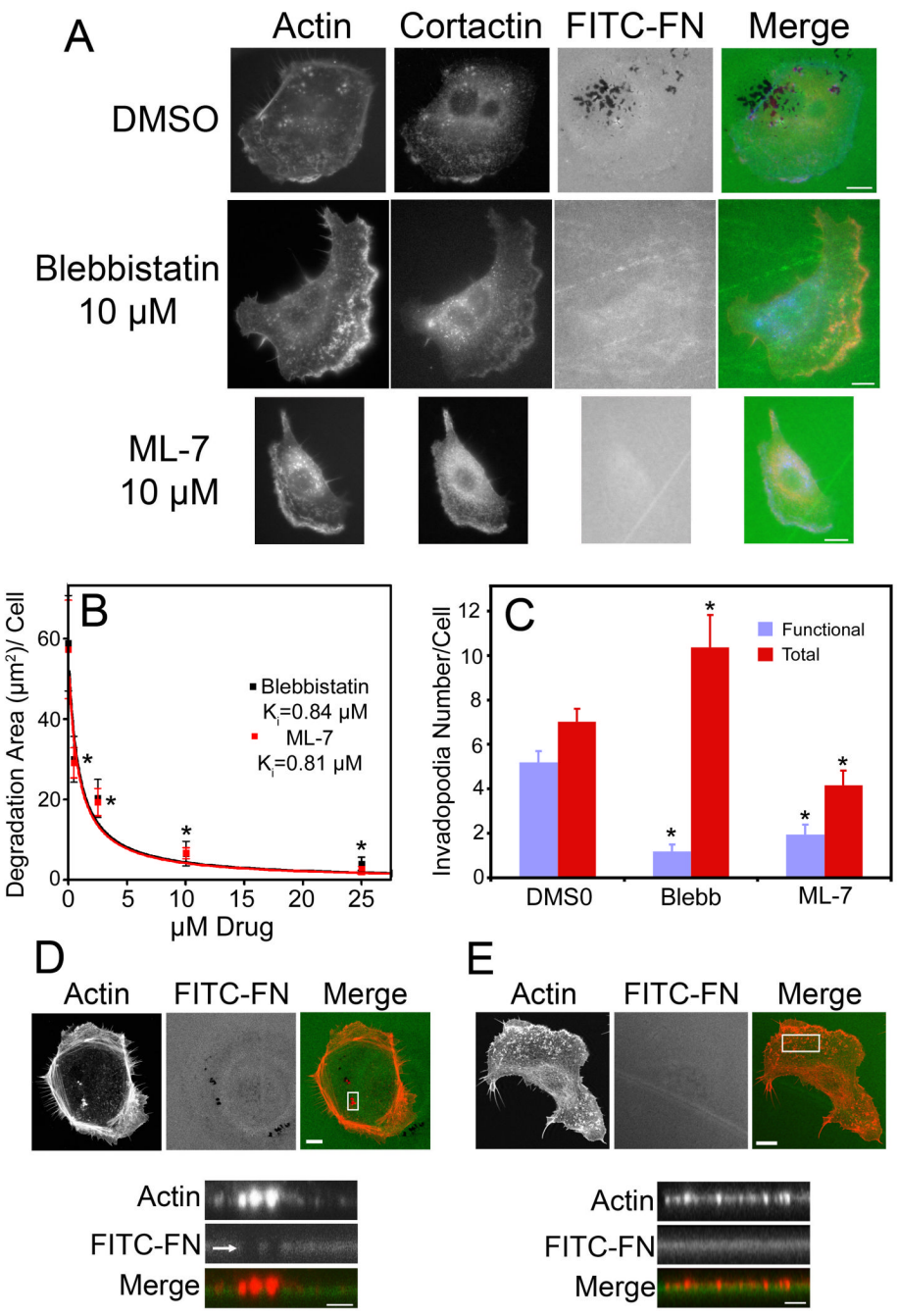

Figure 3. Inhibition of Myosin II activity eliminates invadopodia-associated ECM degradation

A. Images of CA1D cells treated with the myosin inhibitor blebbistatin and the MLCK inhibitor ML-7 after plating on FITC-FN/2.5% gelatin on glass coverslips. **B**. Quantification of the dose dependent inhibition of ECM degradation area/cell following treatment with the indicated doses of blebbistatin or ML-7. Data are represented as mean+/−SE. K_is were determined by fitting the data with standard hyperbolic inhibition curves according to the equation y = constant/(K_i+concentration). **C**. Quantification of the number of total invadopodia (all cortactin/actin-positive puncta) and functional invadopodia (cortactin/actin-positive puncta colocalized with FITC-Fn degradation) in cells treated with 10 μM blebbistatin or ML-7. * indicates p value < 0.05, compared with control cells. **D**. Confocal image of control cell with

invadopodia degrading FITC-FN/gelatin. **E**. Confocal image of a cell treated with 10 μM blebbistatin. For D. & E., the cell areas within the white boxes were further imaged using Z-section analysis. Note that in blebbistatin-treated cells, the actin puncta are smaller and more numerous than in control cells and only protrude partially into the FITC-FN. In addition, unlike in control cells, there is no ECM degradation associated with actin puncta in blebbistatin-treated cells (white arrow in control FITC-FN Z-stack points to ECM degradation). Scale bars are 10 μm for A. and 2 μm for D. & E.

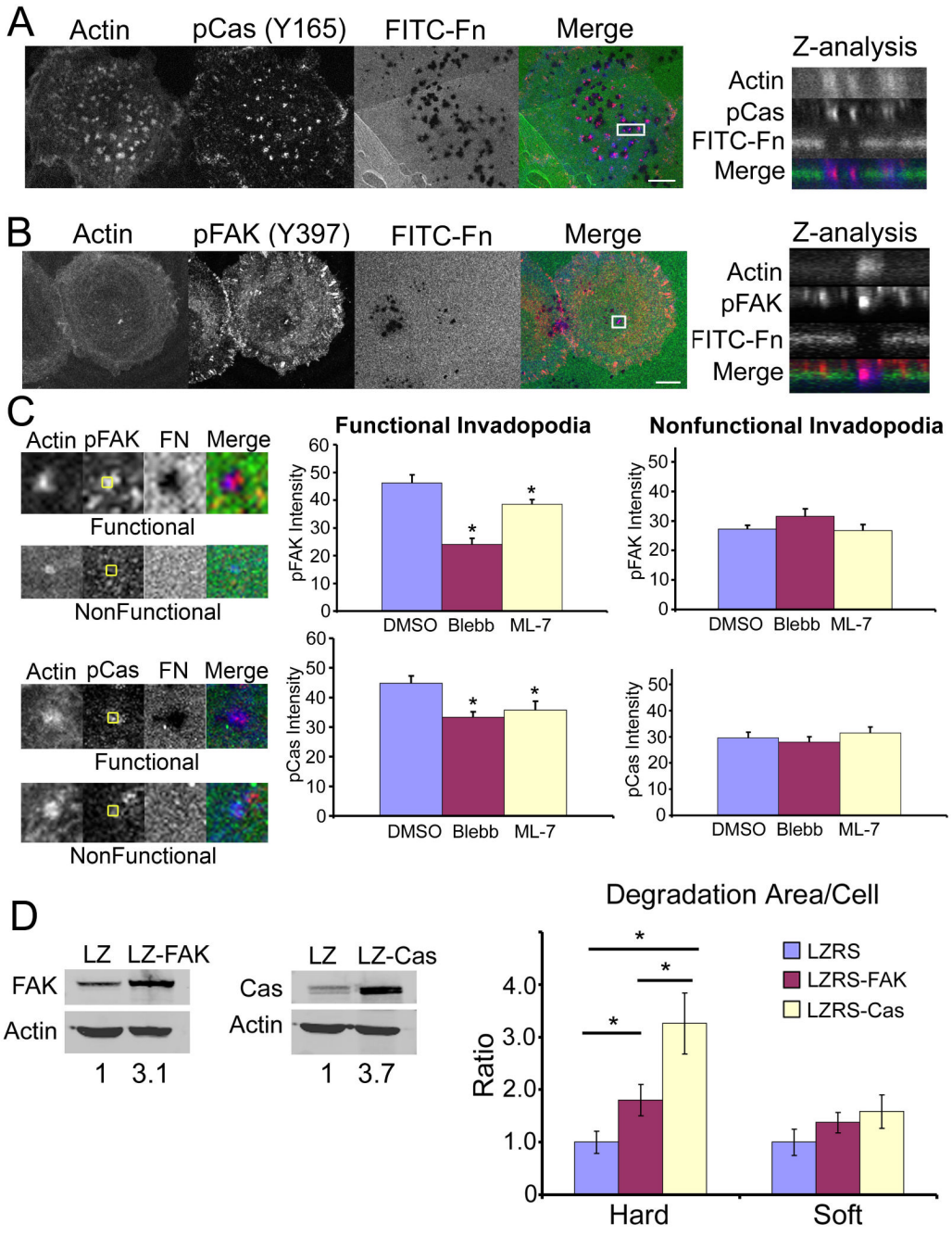

Figure 4. The mechanosensing signaling proteins FAK and p130Cas localize to and regulate invadopodia

A. Confocal immunofluorescent localization of actin filaments (Actin, blue in merges) and phospho-p130cas (Y165, red in merges) to invadopodia. ECM degradation is evident as dark areas on the FITC-fibronectin image (FITC-FN, green in merges). Z-section reconstruction shows that pY165-p130cas (pCas) is present throughout the invadopodia protrusion and colocalizes to areas of ECM degradation. **B**. Confocal immunofluorescent localization of phosphorylated FAK (pFAK (Y397)) to invadopodia. Colors in merges are as in A. White boxes in the merged images indicate areas analyzed in the Z-sections. **C**. Quantitation of phosphoFAK (Y397, “pFAK”) and phosphoCas (Y165, “pCas”) was performed by measuring

absolute intensity of antibody stainings in a 4×4 pixel box (yellow boxes in zoomed images show examples) placed in the center of invadopodia, as defined by punctate actin staining. Functional invadopodia were defined to have associated ECM degradation, whereas nonfunctional did not. For A-C, cells were plated on FITC-Fn overlying 2.5% gelatin. * indicates $p<0.05$. **D**. Overexpression of FAK and Cas was achieved by retroviral transduction of CA1d cells with LZRS-MS-FAK (LZ-FAK) or LZRS-MS-Cas (LZ-Cas) vectors, to achieve a 3.1-fold or 3.7-fold increase in protein expression compared with vector only (LZ) controls (representative Western blots for total FAK or Cas protein shown, along with anti-actin Western loading controls). Degradation area per cell was measured on Hard or Soft PA gels coated with 1% gelatin/TRITC- or FITC-Fn, as in Fig 2. Results are presented as the ratio of degradation area/cell for FAK- or Cas-overexpressing cells compared with LZRS controls and show a strong effect on hard PA gels, but only a trend toward increased degradation with FAK or Cas on soft PA gels. Asterisks indicate $p<0.05$. Statistical significance was calculated from raw data. Error bars were converted: [raw data SEM/raw data mean] × ratio difference. Scale bar = 10 μm.